Journal of Power Sources 195 (2010) 1359–1364

Contents lists available at ScienceDirect

Journal of Power Sources

journal homepage: www.elsevier.com/locate/jpowsour

Short communication

Ni–LnO_x (Ln = La, Ce, Pr, Nd, Sm, Eu, and Gd) cermet anodes for intermediate-temperature solid oxide fuel cells

Beibei He, Dong Ding, Changrong Xia*

CAS Key Laboratory of Materials for Energy Conversion, Department of Materials Science and Engineering, University of Science and Technology of China, Hefei, 230026 Anhui, China

ARTICLE INFO

Article history:
Received 17 July 2009
Received in revised form
15 September 2009
Accepted 15 September 2009
Available online 23 September 2009

Keywords:
Solid oxide fuel cells
Anode
Electrocatalytic activity
Porosity

ABSTRACT

The cermet anodes for solid oxide fuel cells (SOFCs) usually consist of Ni and an oxygen ion conductor such as yttria-stabilized zirconia (YSZ) and doped ceria (DCO). In this work, Ni–LnO_x cermets (Ln = La, Ce, Pr, Nd, Sm, Eu, Gd), in which LnO_x is not an oxygen ion conductor, are primarily investigated as the anodes for intermediate-temperature SOFCs. The electrochemical performances of the Ni–LnO_x anodes are characterized using single SOFCs with $Sm_{0.5}Sr_{0.5}CoO_3$ composite cathodes and $Gd_{0.1}Ce_{0.9}O_{1.95}$ electrolytes. When humidified H_2 is used as the fuel and ambient air as the oxidant, Ni–CeO_2 and Ni–Gd_2O_3 anodes have exhibited very high performance, which is comparable to that of Ni–DCO anodes, the state-of-the-art electrodes for intermediate-temperature SOFCs with ceria electrolytes. The performance is further improved by increasing the anode porosity; peak power density up to 730 mW cm^{-2} and total interfacial polarization resistance down to 0.12 Ω cm^2 are achieved for Ln = Sm, Eu, Ce, and Gd. The low interfacial polarization resistance and high power densities might be related to the high catalytic activity of LnO_x and the optimized microstructures by increasing the porosity. These results suggest a promising alternative to the conventional anodes for SOFCs.

1. Introduction

Solid oxide fuel cells (SOFCs) have received great attention due to their potential for providing a highly efficient and environmentally benign way of generating electricity [1–3]. At the present time, development of anode materials has focused on several classes of materials including Cu cermets [4–6], perovskites [7–9] and pyrochlores [10], etc. But the most advanced SOFCs are clearly those based on the so-called cermet anodes, which are composed of Ni and an oxygen ion conducting ceramic such as yttria-stabilized zirconia (YSZ) or doped ceria (DCO) [11,12]. In these anodes, Ni acts as both the catalyst for electrochemical oxidation of the fuel and electronic conducting phase, while the ceramic possess a substantial oxygen ionic conductivity, so that the reaction zone can be extended from the electrode–electrolyte interface to the bulk of the electrode.

In the case of Ni–YSZ cermets, zirconia additions have been reported to improve the oxidation kinetics without essential influence on the reaction mechanism by expanding the electrochemically active zone up to 10–20 μm from the electrolyte surface due to the ionic transport in the zirconia matrix. When YSZ is replaced by DCO, the kinetics is in principle further improved due to DCO having higher oxygen ion conductivity in combination with higher electrocatalytic activity than YSZ. For example, using YSZ as the electrolyte layer, Ni–$Sm_{0.2}Ce_{0.8}O_{1.9}$ anodes exhibited overpotential of about 25 mV at 800 °C and 200 mA cm^{-2} while Ni–$(Y_2O_3)_{0.08}(ZrO_2)_{0.92}$ anodes displayed 200 mV overpotential under the same conditions [13]. Generally, the higher the oxygen ionic conductivity of the added electrolyte, the lower is the anodic overpotential or the interfacial polarization resistance. This is demonstrated by comparison studies of anode materials with different levels of the oxygen ionic transport, namely, Ni–$Y_{0.15}Zr_{0.85}O_{1.93}$, Ni–$Gd_{0.1}Ce_{0.9}O_{2-\delta}$, $Gd_{0.4}Ce_{0.6}O_{2-\delta}$, $La_{0.75}Sr_{0.25}Cr_{0.97}V_{0.03}O_{3-\delta}$, and $Zr_{0.71}Y_{0.12}Ti_{0.17}O_{2-\delta}$. It confirmed that increasing ionic conductivity leads to lower values of the total polarization resistance [14]. An analogous correlation was also found between the anodic overpotentials and ionic conduction in the cermet anodes made of Ni–SDC, Ni–$Gd_{0.2}Ce_{0.8}O_{2-\delta}$, Ni–$Nd_{0.9}Ca_{0.1}Ga_{0.9}Co_{0.1}O_{3-\delta}$, Ni–$La_{0.9}Sr_{0.1}Ga_{0.8}Mg_{0.115}Co_{0.085}O_{3-\delta}$, Ni–$Gd_2Ti_2O_7$, and pure Ni [15].

In addition to the reaction zone expansion, oxide components have also a number of important functions, including matching thermal expansion of the cell components, stabilizing the anode layer with respect to redox cycling, preventing sintering of metal particles, and acting as catalyst or catalyst support. Consequently, it is often impossible to separate the effects originating from ionic conduction in the oxide phase from changes in the catalytic behavior and anode microstructure. In some cases, catalytic activity is

* Corresponding author. Tel.: +86 5513607475; fax: +86 5513601592.
E-mail address: xiacr@ustc.edu.cn (C. Xia).

0378-7753/$ – see front matter © 2009 Elsevier B.V. All rights reserved.
doi:10.1016/j.jpowsour.2009.09.035

more important than the oxygen ion conductivity. Recently, the Ni–Sm_2O_3 cermet anodes have been shown to have performance comparable to that of Ni–SDC anodes for intermediate-temperature SOFCs [16], even though ionic conductivity of Sm_2O_3 is negligible comparing with SDC. The high cell performance is possibly due to the high catalytic activity of Sm_2O_3.

Here, lanthanide oxides (La_2O_3, CeO_2, Pr_6O_{11}, Nd_6O_{11}, Sm_2O_3, Eu_2O_3, and Gd_2O_3) are primarily investigated as the ceramic components for Ni-based anodes. The oxides are cooperated with NiO to form NiO–LnO_x composites, which are in situ reduced to Ni–LnO_x and characterized using single cells based on $Gd_{0.1}Ce_{0.9}O_{1.95}$ electrolytes and $Sm_{0.5}Sr_{0.5}CoO_3$ composite cathodes.

2. Experimental

2.1. Cell fabrication

Oxide powders involved in this work including lanthanide oxides (LnO_x), NiO, $Gd_{0.1}Ce_{0.9}O_{1.95}$ (GDC, the electrolyte material) and $Sm_{0.5}Sr_{0.5}CoO_3$ (SSC, the cathode material) were synthesized via a glycine–nitrate process (GNP) [17] with nitrates as the starting materials. The nitrates and glycine were dissolved in distilled water to form a solution with the mole ratio of glycine/metal of 2:1. The solution was then heated till self-combustion occurred. The resulted ash was heated at 800 °C for 2 h to form oxide powders. X-ray diffraction analysis showed that lanthanide oxides were in the form of La_2O_3, CeO_2, Pr_6O_{11}, Nd_6O_{11}, Sm_2O_3, Eu_2O_3, and Gd_2O_3. A mixed powder of NiO and lanthanide oxides (in a weight ratio of NiO:LnO_x = 60:40) was pressed at 20 MPa as anode substrates with a diameter of 13 mm. Samples with 20 wt.% spherical graphite as pore former were also prepared for comparison. GDC powder was then added, distributed uniformly, and co-pressed [18] onto the substrate at 280 MPa. The bilayer was subsequently sintered at 1150 °C for 5 h to burn out the graphite and result in a dense GDC film on the NiO–LnO_x substrate. In order to evaluate the catalytic activity of Ni–LnO_x as the anode, for comparison, single cells with Ni–GDC and Ni–Al_2O_3 as the anodes were also fabricated with the same process. Al_2O_3 is non-active for any catalytical oxidation reaction. SSC–SDC (in a weight ratio of SSC:SDC = 70:30) powders were mixed thoroughly with a 10 wt.% ethylcellulose–terpineol binder to prepare cathode slurry. The slurry was painted on the GDC electrolyte layers and fired at 950 °C for 2 h to form single cells. The fabricating process was kept as consistent as possible so that identical cathodic polarization resistance could be achieved. The thickness of the electrolyte and anode was about 30 μm and 0.4 mm, respectively. The single cell with Ni–LnO_x as the anode is designated as FC–LnO_x. For example, FC–La_2O_3 represents a single cell with a Ni–La_2O_3 anode, a GDC electrolyte, and an SSC–SDC cathode. The average grain size of the anode support was ~2.6 μm as estimated with scanning electron microscopy. And the measured average pore diameter of the anode support was ~1.3 μm as measured with mercury porosimetry.

2.2. Cell testing and microstructure characterization

The single cells were sealed onto alumina tubes with silver paste (DAD-87, Shanghai Research Institute of Synthetic Resins). Humidified (3% H_2O) hydrogen was used as the fuel with a flow rate of 50 mL min^{-1} and ambient air as the oxidant. NiO was in situ reduced to Ni at 600 °C for 2 h. An Electrochemical Workstation (IM6e, Zahner) was used to characterize the single cells. The current–voltage curve was obtained by using a galvanostat mode and the electrochemical impedance spectra were measured under open-circuit conditions in the frequency range typically from 0.1 Hz to 1 MHz. The porosity and pore size distribution of the anode was measured with mercury porosimetry (Poremaster GT-60). The phase identification of porous NiO–LnO_x substrates was conducted with X-ray diffraction (XRD) analysis using Cu Kα radiation (D/Max-gA) at room temperature. The microstructure was observed via a scanning electron microscope (SEM, JSM-6700F, JEOL).

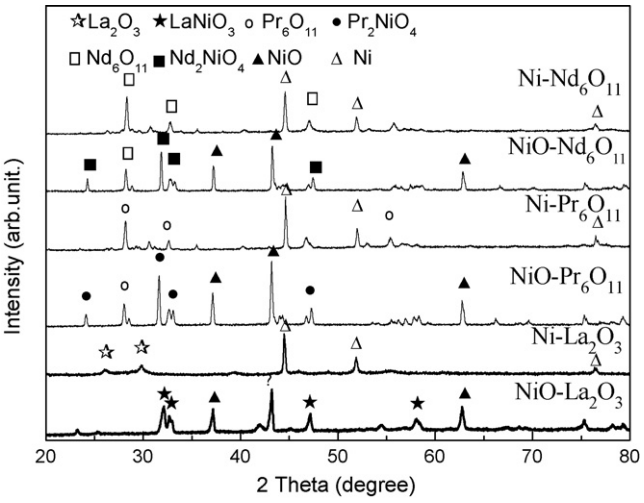

Fig. 1. XRD patterns of NiO–LnO_x and Ni–LnO_x composites (Ln = La, Pr and Nd). NiO–LnO_x was sintered at 1150 °C for 5 h and Ni–LnO_x was formed by reducing NiO–LnO_x at 600 °C with humidified H_2.

3. Results and discussion

3.1. Ni–LnO_x (LnO_x = La_2O_3, Pr_6O_{11} and Nd_6O_{11})

Fig. 1 shows the XRD patterns of NiO–LnO_x and Ni–LnO_x composites, in which LnO_x = La_2O_3, Pr_6O_{11}, and Nd_6O_{11}. Significant reactions took place between NiO and LnO_x when the composites were co-fired at 1150 °C for 5 h in air. The reactions resulted in new compounds; perovskite structured $LaNiO_3$, K_2NiF_4 type structure of Pr_2NiO_4 and Nd_2NiO_4, respectively. These are consistent with previous studies by Zaghrioui et al. [19], who synthesized the compounds with NiO and LnO_x at 1350 °C using a solid-state reaction method. Diffraction peaks corresponding to NiO also present on the patterns, indicating the reactions have not consumed all the NiO since the NiO to LnO_x weight ratio was 60:40 in the starting materials. It looks very likely that La_2O_3 reacts completely with NiO while the reaction between Pr_6O_{11} or Nd_6O_{11} and NiO is not complete in the cell fabricating conditions. When the NiO–LnO_x composites were treated at 600 °C for 10 h with humidified H_2, NiO was reduced to Ni as expected. The treatment also had effect on the newly formed compounds; $LaNiO_3$ decomposed to La_2O_3, Nd_2NiO_4 to Nd_6O_{11}, and Pr_2NiO_4 to Pr_6O_{11} (Fig. 1).

Fig. 2a shows the cell performance when the NiO–LnO_x composites were in situ reduced and used as the anodes. A cell based on a Ni–GDC composite anode, which was prepared with the same fabrication procedure, is also tested for comparison. The performance of FC–GDC is similar to those reported in the literature with Ni–SDC or Ni–GDC anodes, which usually generate peak power density of about 400 mW cm^{-2} at 600 °C [17,18,20–22]. Peak power densities at 600 °C are only 160, 176 and 154 mW cm^{-2} for FC–La_2O_3, FC–Pr_6O_{11}, and FC–Nd_6O_{11}, respectively. The power densities are much lower than that of FC–GDC, which generates peak power density of about 457 mW cm^{-2} at 600 °C. The relatively low power densities suggest poor activity of Ni–La_2O_3, Ni–Pr_6O_{11} and Ni–Nd_6O_{11} anodes. Fig. 2b is impedance spectra measured under open-circuit conditions. The total interfacial polarization resistance, which is derived from the difference between

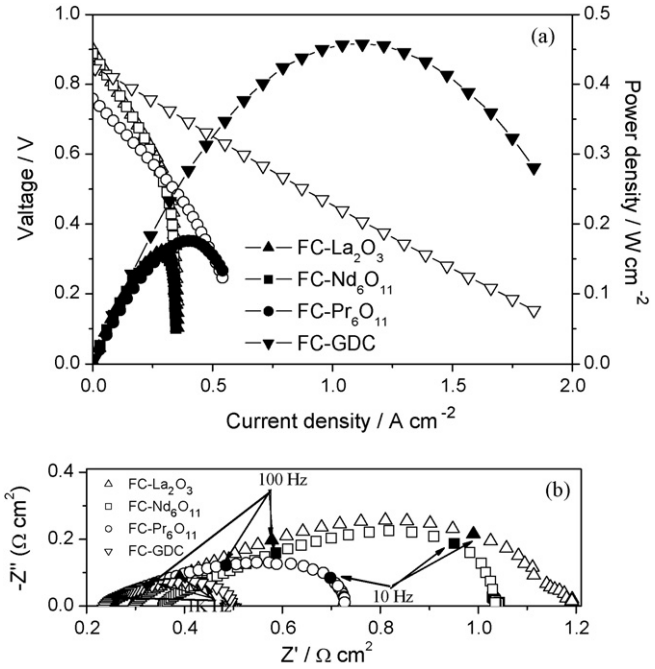

Fig. 2. (a) I–V curves measured at 600 °C for the single cells with Ni–LnO_x (Ln = La, Pr, and Nd) and Ni–GDC anodes and (b) impedance spectra at the same temperature measured under open-circuit conditions.

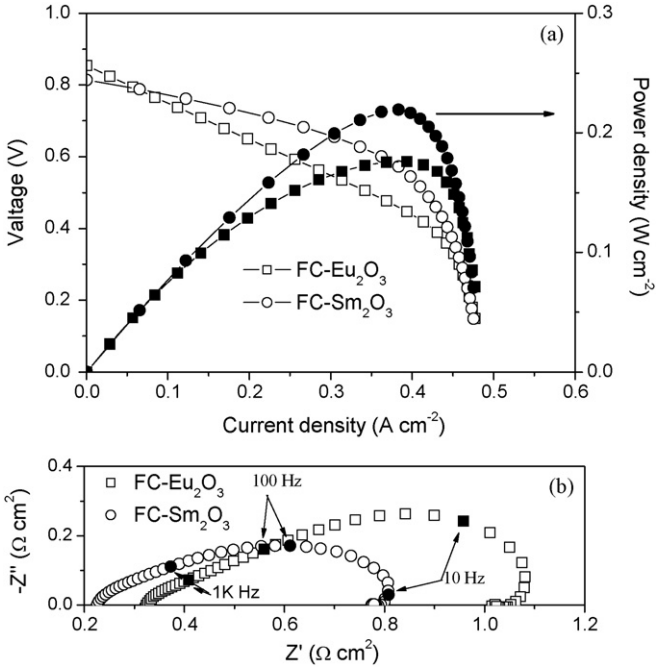

Fig. 4. (a) I–V curves measured at 600 °C for single cells with Ni–LnO_x (Ln = Sm, Eu) anodes and (b) impedance spectra measured at the same temperature under open-circuit conditions.

low and high frequency intercepts at the real axis, is 0.90, 0.48 and 0.68 Ω cm^2, respectively. The resistances are much higher than the typical value of 0.2 Ω cm^2 reported for Ni–SDC and Ni–GDC based fuel cells [17,18,20–22]. They are also higher than that for FC–GDC, 0.25 Ω cm^2 (Fig. 2b). Since the cathodes have the same composition and are fabricated with the same process, the resistance associated with the cathodic polarization process should be very close for FC–LnO_x and FC–GDC. Therefore, the high resistance should be attributed to the low electrochemical activity of Ni–La_2O_3, Ni–Pr_6O_{11} and Ni–Nd_6O_{11} anodes. In addition to the high interfacial polarization resistances under open-circuit conditions, FC–La_2O_3 and FC–Nd_6O_{11} exhibited high concentration polarization when current density was higher than 0.3 A cm^{-2}. The poor anodic performance might due to solid-state reactions occurred between NiO and LnO_x in the cell fabrication process although NiO was subsequently released and reduced to Ni under fuel-cell operation conditions. Because of the poor performance and solid-state reaction, the three lanthanide oxides could not be good candidates as SOFC anode materials.

3.2. Ni–LnO_x (LnO_x = Sm_2O_3 and Eu_2O_3)

Fig. 3 is the XRD patterns of NiO–LnO_x (LnO_x = Sm_2O_3 and Eu_2O_3) and their reduced products. Unlike La_2O_3, Nd_6O_{11} and Pr_6O_{11}, Sm_2O_3 and Eu_2O_3 do not react with NiO to form any new compounds when they are sintered at 1150 °C for 5 h. Although Eu_2O_3 is compatible with NiO, it changes its crystal structure from monoclinic with a space group C2/m(1 2) to cubic fluorite with a space group $Ia\bar{3}$(206) when it is treated at 600 °C with humidified H_2. So does Sm_2O_3, which partly changes to cubic phase from monoclinic structure. Single cells with Ni–Sm_2O_3 and Ni–Eu_2O_3 composite anodes generate peak power densities of 219 and 176 mW cm^{-2}

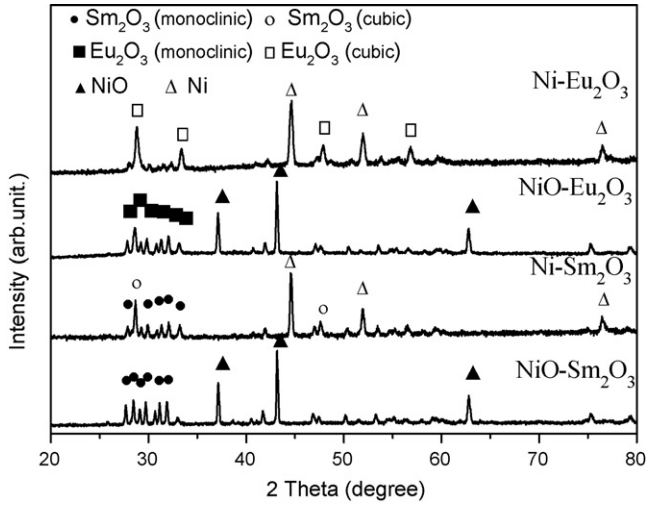

Fig. 3. XRD patterns of NiO–LnO_x and Ni–LnO_x composites (Ln = Sm, Eu).

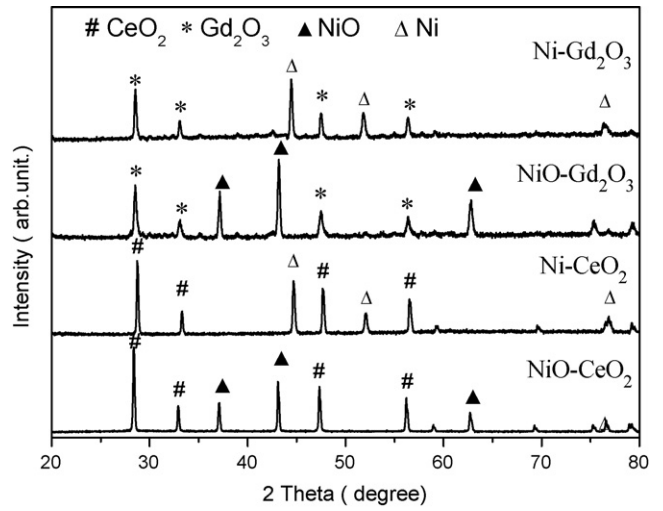

Fig. 5. XRD patterns of NiO–LnO_x and Ni–LnO_x composites (Ln = Ce, Gd).

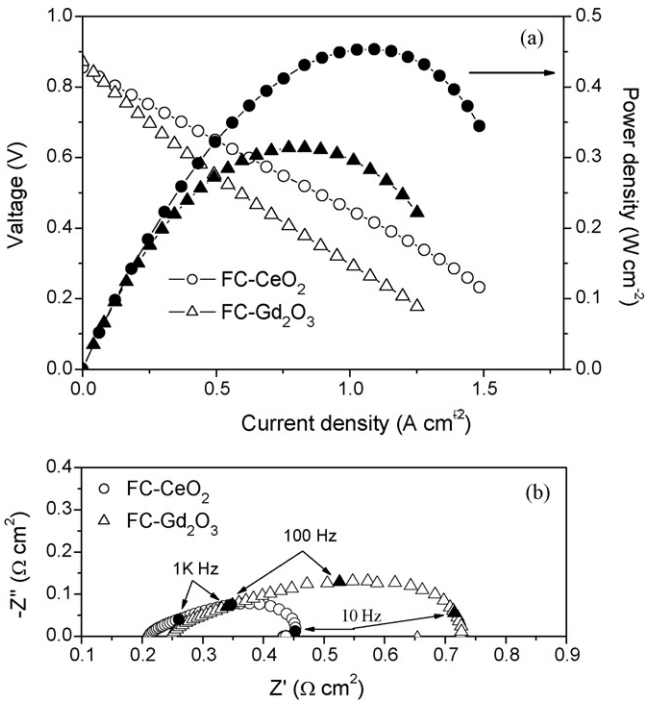

Fig. 6. (a) I–V curves measured at 600 °C for the single cells with Ni–LnO_x (Ln = Ce, Gd) anodes and (b) impedance spectra measured at the same temperature under open-circuit conditions.

at 600 °C (Fig. 4a), respectively. The interfacial polarization resistances under open-circuit conditions are 0.55 and 0.70 Ω cm^2 (Fig. 4b), respectively. Concentration polarization is observed when the current density is over 0.4 A cm^{-2}. The cell performance as well as the anodic activity is also lower than those derived from Ni–GDC

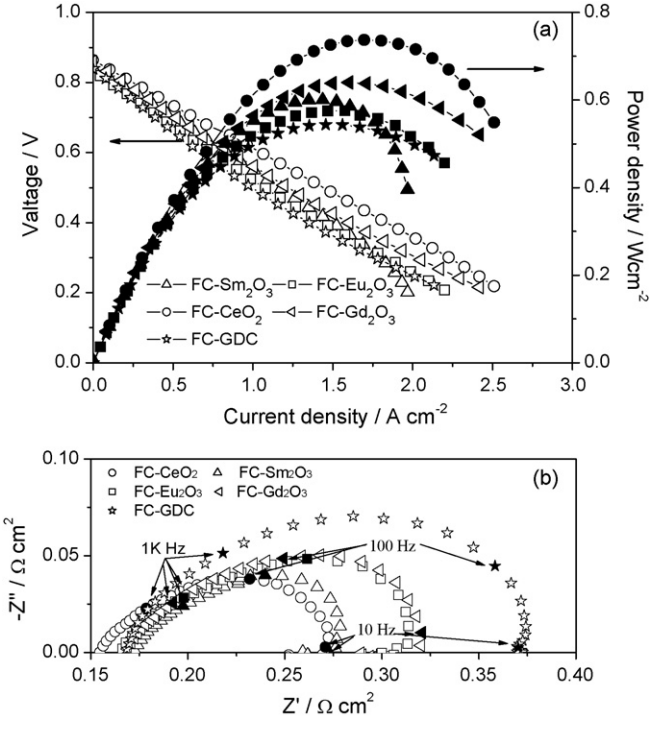

Fig. 7. (a) Cell voltages and power densities as a function of current density measured at 600 °C for fuel cells based on Ni–LnO_x (Ln = Sm, Eu, Ce, Gd) and Ni–GDC anodes when pore former was used. (b) Impedance spectra measured at the same temperature under open-circuit conditions.

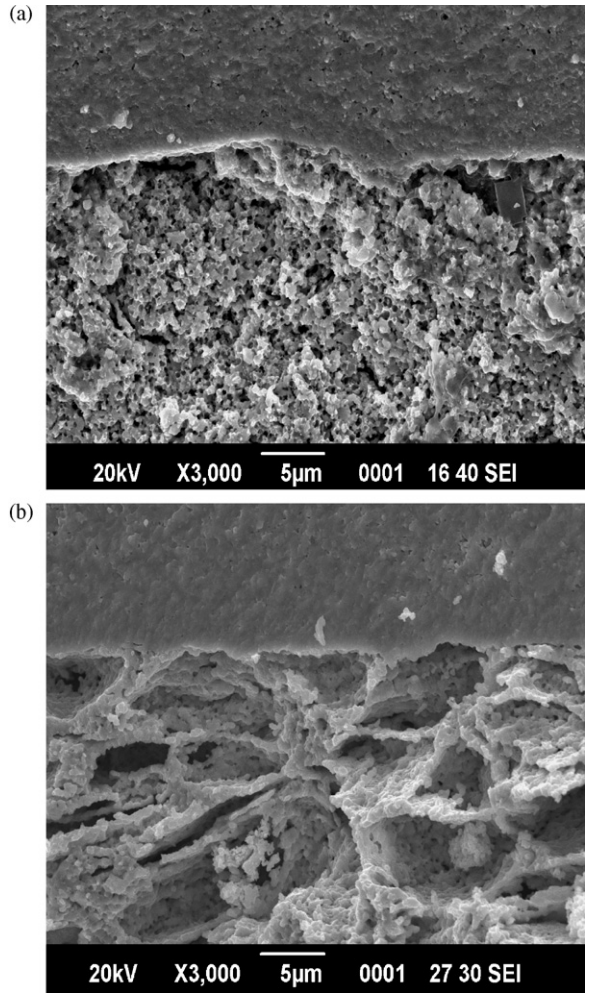

Fig. 8. Cross-sectional views (SEM micrographs) of GDC–electrolyte and Ni–Sm_2O_3 anode components after fuel-cell performance testing. (a) Ni–Sm_2O_3 anodes prepared without pore formers. (b) Ni–Sm_2O_3 anodes prepared with pore formers.

anodes. Phase change might be the reason for the relatively low power export associated with concentration polarization.

3.3. Ni–LnOx (LnOx = CeO_2 and Gd_2O_3)

Fig. 5 shows the XRD patterns of NiO–LnO_x and Ni–LnO_x composites, in which LnO_x = CeO_2 and Gd_2O_3. No solid solutions are formed between NiO and either of the two oxides when they are sintered at 1150 °C for 5 h. When NiO–LnO_x composites are treated at 600 °C with hydrogen, NiO is reduced to Ni. Meanwhile, no obviously phase changes occur. FC–CeO_2 and FC–Gd_2O_3 produce peak power densities of 545 and 314 mW cm^{-2} (Fig. 6a), while the interfacial polarization resistances are 0.23 and 0.48 Ω cm^2 (Fig. 6b), respectively. The exhibited performances are much higher than those of FC–La_2O_3, FC–Pr_6O_{11}, FC–Nd_6O_{11}, FC–Sm_2O_3, and FC–Eu_2O_3. In addition, the performance is consistent with our previous results [16]. It seems that the performance is critically related to the stability of LnO_x when it is used as the anode component. Both solid-state reaction in cell fabrication processes and phase change in the process when NiO is reduced to Ni might cause deteriorating electrochemical performance. Unlike Gd_2O_3, which is chemically stable under anodic conditions, CeO_2 can be partially reduced, $Ce^{4+} = Ce^{3+} + e$, resulting in some ionic mobility as well as a degree of electronic conductivity. The reduction and its associated ionic and electronic conduction might be other reasons for the high performance of FC–CeO_2.

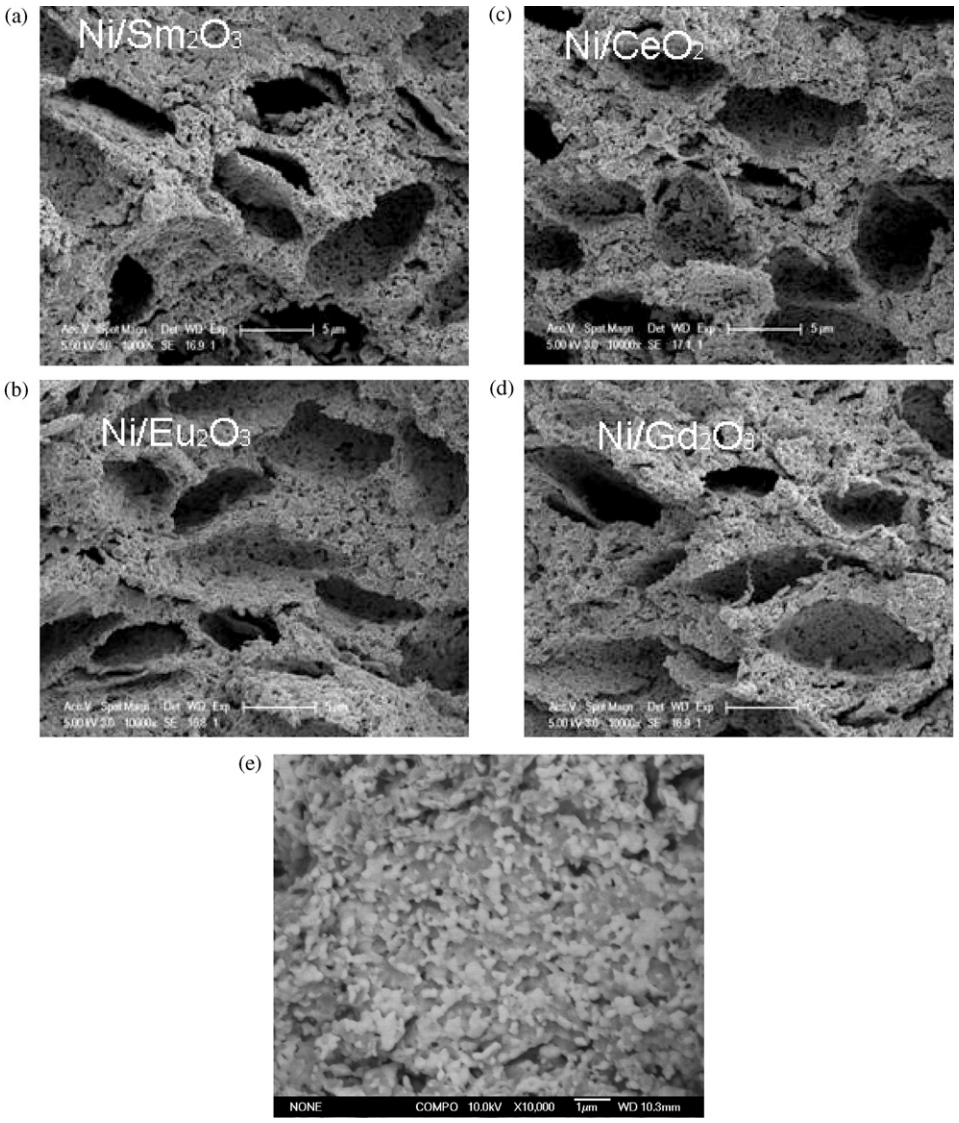

Fig. 9. (a)–(d) SEM micrographs for cross-section views of NiO–LnO_x (LnO_x = Sm_2O_3, Eu_2O_3, CeO_2, Gd_2O_3) anodes prepared with pore formers. (e) EBSD micrographs of cross-section for Ni–Gd_2O_3 anode.

3.4. Effect of anode porosity

Concentration polarization is observed although no solid-state reaction occurs between NiO and Sm_2O_3 or Eu_2O_3. So, it is very likely that phase changes might be the reason for the concentration polarization, which is usually due to the low porosity of electrodes. The polarization might be minimized by increasing the anode porosity. In order to investigate the effect of anode porosity on fuel-cell performance, spherical graphite of 20 wt.% to NiO–LnO_x was added as the pore former. Fig. 7a shows typical current–voltage curves at 600 °C for FC–Sm_2O_3, FC–Eu_2O_3, FC–CeO_2 and FC–Gd_2O_3 that are prepared with the pore former. FC–GDC prepared with pore former is also shown for comparison. The open-circuit voltages (OCVs) are in the range of 0.84–0.87 V, close to those with Ni–GDC anodes and GDC electrolytes. The peak power densities are 600, 575, 738, and 640 mW cm^{-2}, respectively, higher than that of 544 mW cm^{-2} obtained with FC–GDC when pore former is used. Cell performances of FC–Sm_2O_3 and FC–Eu_2O_3 are relatively lower than those of FC–CeO_2 and FC–Gd_2O_3, which could be caused by the phase change of Sm_2O_3 and Eu_2O_3. However, the power densities are higher than that prepared without pore former (Fig. 4a). Shown in Fig. 8 is the microstructure comparison of Ni–Sm_2O_3 anodes prepared with and without graphite addition. In both cases, the GDC electrolyte is strongly attached to the anodes and shows a well defined interface. It can be seen that the use of pore former has increased not only the porosity but also pore size. The anode without using pore former has small pores about 1–2 μm in size, whereas the anodes prepared with pore former has not only the small pores but also big pores, about 10 μm in size. The difference between the power densities shown in Fig. 4a and Fig. 7a is most possibly due to the microstructure difference of the anodes (Fig. 8). Therefore, the performance of FC–Sm_2O_3 and FC–Eu_2O_3 can be substantially improved by increasing the anode porosity.

Fig. 7b shows the impedance spectra under open-circuit conditions. The ohmic resistances of FC–LnO_x (LnO_x = Sm_2O_3, Eu_2O_3, CeO_2, and Gd_2O_3) corresponding to the real axis intercepts at high frequency, are 0.171, 0.171, 0.161, and 0.171 Ω cm^2, which are very close to each other. The total interfacial polarization resistances are 0.081, 0.131, 0.121, and 0.121 Ω cm^2, respectively, lower than the value of 0.20 Ω cm^2 for FC–GDC prepared with pore former, and much lower than those obtained without graphite addition.

The electrochemical performance of an anode depends on the catalytic activity of the materials and its microstructure characteristics including porosity. It has been revealed that Ni–LnO_x

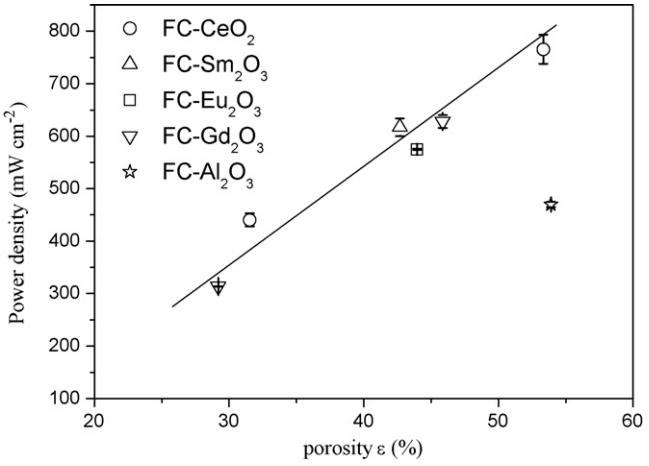

Fig. 10. The peak power densities measured at 600 °C at different anode porosity for cells FC–Sm_2O_3, FC–Eu_2O_3, FC–CeO_2, FC–Gd_2O_3 and FC–Al_2O_3.

composites (Ln = La, Ce, Pr, Nd, Sm, Eu, and Gd) have shown high activity in the oxidative conversion of methane to sygas [23]. These catalysts differ in activity from each other but only to a small extent. Therefore, the catalytic of the Ni–LnO_x anodes is reasonably assumed to be close to each other. The microstructure of the Ni–LnO_x (Ln = Sm, Eu, Ce, and Gd) anodes prepared with graphite are also similar. Fig. 9 shows their cross-sectional micrographs for the samples that have been used for performance test. These anodes display very similar microstructures; pores with size up to 10 μm present in the anodes, the particles of Ni and LnO_x are very fine and have similar size, which is far smaller than the pore size. As can be seen from Fig. 9e, the two phases (Ni and LnO_x) are uniformly distributed and well connected. This characteristic is desirable for both catalytic reaction and electronic conduction. For the Ni–Gd_2O_3 anode, it is clearly seen that the Gd_2O_3 forming isolated fine grains, and the dark one (Ni particles) are uniformly distributed and well connected. It is noted that although the microstructures are similar to each other, Ni–CeO_2 has the highest porosity, which might due to different sintering behavior of NiO–LnO_x. Simultaneously, FC–CeO_2 has the highest power density and lowest interfacial polarization resistance as shown in Fig. 7.

Fig. 10 shows the peak power density versus Ni–LnO_x porosity. The porosity is high enough so that concentration polarization is negligible. The power density increases almost linearly with the porosity, indicating the porosity has a determine effect on the performance of Ni–LnO_x anodes. It also infers that the electrochemical activity of LnO_x is very similar for Ln = Sm, Eu, Ce, and Gd when the Ni–LnO_x anode is free of concentration polarization. This agrees well with the previous report by Choudhary et al, who have demonstrated that LnO_x have similar activity for oxidation [23,24]. The electrochemical activity of LnO_x is further illustrated with single cells using Ni–Al_2O_3 as the anode (Fig. 10). The power density of FC–Al_2O_3 is much lower than that of FC–CeO_2 although the two cells have similar porosities. Al_2O_3 is believed to be not active for oxidation reactions. Choudhary et al. have also demonstrated that Ni–LnO_x catalysts are much superior to Ni–Al_2O_3 in the oxidative conversion of methane to sygas [23]. It should be noted that the different porosity is obtained although NiO–LnO_x is fabricated with the same procedure, which infers the different sintering behavior of LnOx.

The performance of a Ni–cermet anode depends usually on the conductivity of its ceramic component. However, this work demonstrates that when the catalytic activity is high enough, the oxygen ionic conductivity might not so important. In addition to the catalytic activity, the porosity might be more critical than that has been ever considered. Therefore, the difference in electrochemical performance might be directly related to the porosity of the anode.

4. Conclusions

Ni–LnO_x (Ln = La, Ce, Pr, Nd, Sm, Eu, and Gd) composite are preliminary investigated as the anodes for solid oxide fuel cells. When Ln = La, Pr, and Nd, the cells have shown very low performance, which might be caused by the solid-state reactions between NiO and La_2O_3, Pr_6O_{11} or Nd_6O_{11} during the cell fabrication processes. When Ln = Sm and Eu, the anodes performance is limited by concentration polarization, which is possibly caused by phase change of Sm_2O_3 and Eu_2O_3 as well as the low anodes porosity. When Ln = Ce and Gd, high performance is achieved. The performance is comparable to that reported for Ni–DCO anodes, and can be further improved by increasing the anode porosity. When the porosity is high enough to eliminate concentration polarization, the Ni–LnO_x (Ln = Ce, Sm, Eu, and Gd) anodes exhibit very high performance; power density over 600 mW cm^{-2} is achieved at 600 °C with these anodes. These results suggest new anode materials for SOFCs.

Acknowledgements

This work was supported by the Natural Science Foundation of China (50672096 and 50730002) and the Ministry of Science and Technology of China (2007AA05Z151).

References

[1] Z.P. Shao, S.M. Haile, Nature 431 (2004) 170–173.
[2] T. Norby, Solid State Ionics 125 (1999) 1–11.
[3] S. McIntosh, R.J. Gorte, Chem. Rev. 104 (2004) 4845–4865.
[4] O. Costa-Nunes, R.J. Gorte, J.M. Vohs, J. Power Sources 141 (2005) 241–249.
[5] D.P. Fagg, G.C. Mather, J.R. Frade, Ionics 9 (2003) 214–219.
[6] H.P. He, R.J. Gorte, J.M. Vohs, Electrochem. Solid State Lett. 8 (2005) A279–280.
[7] G. Pudmich, B.A. Boukamp, M. Gonzalez-Cuenca, W. Jungen, W. Zipprich, F. Tietz, Solid State Ionics 135 (2000) 433–438.
[8] S. Primdahl, J.R. Hansen, L. Grahl-Madsen, P.H. Larsen, J. Electrochem. Soc. 148 (2001) A74–81.
[9] F.J. Lepe, J. Fernandez-Urban, L. Mestres, M.L. Martinez-Sarrion, J. Power Sources 151 (2005) 74–78.
[10] E.V. Tsipis, V.V. Kharton, J.R. Frade, J. Eur. Ceram. Soc. 25 (2005) 2623–2626.
[11] B. de Boer, M. Gonzalez, H.J.M. Bouwmeester, H. Verweij, Solid State Ionics 127 (2000) 269–276.
[12] M. Watanabe, H. Uchida, M. Yoshid, J. Electrochem. Soc. 144 (1997) 1739–1743.
[13] C.J. Wen, T. Masuyama, T. Yoshikawa, J. Otomo, H. Takahashi, K. Eguchi, K. Yamada, in: H. Yokokawa, S.C. Singhal (Eds.), SOFC-VII, vol. 16, Pennington, NJ, 2001, p. 671.
[14] S. Primdahl, M. Mogensen, Solid State Ionics 152 (2002) 597–608.
[15] T. Ishihara, T. Shibayama, H. Nishiguchi, Y. Takita, Solid State Ionics 132 (2000) 209–216.
[16] D. Ding, L. Li, K. Feng, Z.B. Liu, C.R. Xia, J. Power Sources 187 (2009) 400–402.
[17] C.R. Xia, W. Rauch, F.L. Chen, M.L. Liu, Solid State Ionics 149 (2002) 11–19.
[18] C.R. Xia, M.L. Liu, J. Am. Ceram. Soc. 84 (2001) 1903–1905.
[19] M. Zaghrioui, F. Giovannelli, N. Poirot, D. Brouri, I. Laffez, J. Solid State Chem. 177 (2004) 3351–3358.
[20] S.W. Zha, William Rauch, M.L. Liu, Solid State Ionics 166 (2004) 241–250.
[21] R. Doshi, V.L. Richards, J.D. Carter, X. Wang, M. Krumpelt, J. Electrochem. Soc. 146 (1999) 1273–1278.
[22] C. Xia, M. Liu, Solid State Ionics 144 (2001) 249–255.
[23] V.R. Choudhary, V.H. Rane, A.M. Rajput, Catal. Lett. 22 (1993) 289–297.
[24] A.G. Dedov, A.S. Loktev, I.I. Moiseev, A. Aboukais, J.F. Lamonier, I.N. Filimonov, Appl. Catal. A: Gen. 245 (2003) 209–220.